Available online at https://ifejost.oauife.edu.ng

IFE JOURNAL OF SCIENCE AND TECHNOLOGY

Vol 7. No. 1 (2023) 46–63

Utilization of pectin isolated from tangerine (*Citrus reticulata*) peels as an adsorbent for the confiscation of toxic crystal violet dye from aqueous solution

K. N. Awokoya[1*], V. O. Oninla[1], M. O. Owolabi[1], A. J. Ogunbadeniyi[1], and G. C. Adeyinka[2]

[1]Department of Chemistry, Obafemi Awolowo University, Ile-Ife 220284, Nigeria

[2]Department of Chemical Engineering, Mangosuthu University of Technology, Umlazi, Durban 4001, South Africa

*Corresponding Author: knawokoya@oauife.edu.ng; knawokoya@gmail.com

Telephone: +234(0)8034199393

Abstract

Pectin membrane (PMB) isolated from locally available agricultural waste, tangerine peels (TPP), for application as an adsorbent to remove crystal violet dye (CV) from an aqueous medium. The adsorbent was characterized by different methods for surface morphology, functional groups, and crystal structure composition. The adsorptive removal of CV onto PMB was evaluated across different parameters such as pH, adsorption kinetics, rate-controlling step, isotherm, and thermodynamics. The PMB exhibited high adsorption efficiency towards CV at pH 4 (99.83%) and fast removal rate at 20 min (97.82%). Adsorption kinetic and equilibrium data were well described by the pseudo-second-order and Freundlich isotherm models, suggesting multiple-layer adsorption. The Langmuir maximum adsorption capacity was 133.69 mg g-1, which was much higher than the 13.554 mg g-1 recorded with the control adsorbent (TPP). Additionally, thermodynamic investigations revealed that it was a spontaneous and endothermic process presumably relying on chemisorption. Regeneration studies showed that the dye removal percentages ranged from 93.56 to 95.04% up to four adsorption-desorption cycles. Moreover, in comparison of PMB with other biosorbents, it was found to be highly efficient and could be used as a suitable alternative for adsorbing CV from an aqueous medium.

Keywords: Pectin, tangerine peels, adsorption, crystal violet, wastewater, reusability

Introduction

Rapid population growth all over the world has given rise to both economic growth and industrial development. That being said, this industrial development has brought about the occurrence of toxic substances (organic and inorganic) in most water bodies, thus having some adverse impacts on the overall ecosystem (Wang *et al*., 2008; Awokoya *et al*., 2022).

Some of these adverse impacts on the environment are associated with the increasing generation and haphazard release of sewage and untreated industrial effluents such as synthetic dyes, heavy metals, and many other toxic substances into water bodies (Muntean *et al*., 2013). Amongst these industrial effluents, synthetic dyes provide up to 20% of the global water pollution, causing serious environmental and debilitating health effects such as heavy coloring of water, cancers, mutations, allergic dermatitis, skin irritation, and eye diseases (Zhang *et al*., 2015; Shokrollahi *et al*., 2011). Hence, it is of great importance to remove these toxin-producing dyes from wastewater before it is discharged into the environment. Crystal violet (CRV) dye is a cationic dye with the general formula of CRV that has found applications in textile, leather, and paper dying, also used to colourize various products such as detergent, fertilizer, and nontoxic DNA stain as a substitute to fluorescent (Auerbach *et al*., 2010). Nowadays, several techniques have been proposed for the removal of dyes from wastewater, such as ozonation, oxidation, reverse osmosis, electro-dialysis, precipitation, irradiation, membrane separation, cloud point extraction coagulation, flotation, sedimentation, adsorption, biological (aerobic or anaerobic treatment), etc (Babu *et al*., 2007; Awokoya *et al*., 2013; Salahi *et al*., 2014; Zewail and Yousef, 2015; Srivastav and Roy, 2016; Saini, 2017; Shahedi *et al*., 2020; Awokoya *et al*., 2021; Hamad and Idrus, 2022). Some levels of success have been recorded using all these methods. Nonetheless, with the omission of the adsorption method, all other water remediation methods have their limitations which include high cost of operation, generation of secondary sludge, needless use of chemicals, and low selectivity (Shahedi *et al*., 2020; Saini, 2017). Adsorption is a surface process technology where particles (dyes or other toxic materials) are attached to the surface of porous solid adsorbents (Basheer, 2018). The adsorption process has the superiority of low cost, easy to design, high removal rate, and economical and adsorbent reusability over other methods (Noreen *et al*., 2020; Bautista, *et al*., 2007). Thence, a variety of porous adsorbents and synthetic composite materials such as milk bush kernel shells, coconut husk, spent tea leaves, corn cobs, pine apple stem, garlic peel, rice husk, flamboyant pod, coal, imprinted polymer, carbon nanotubes, activated carbon, clays and various zeolites are used for removal of dye from wastewater (Burakov *et al*., 2018; Kaushal and Singh, 2017). In comparison with other adsorbents, the use of bio-based materials as adsorbents has shown to be economically viable and technically efficient for the removal of dyes from wastewater under various conditions, whilst also accomplishing the recycling of agricultural waste (Noreen *et al*., 2020). Tangerine (*Citrus reticulata L.)* is a seasonal citrus fruit in Nigeria, and belongs *to the Rutaceae family. The peels of Citrus reticulata* are discarded as waste. The citrus peel contains various compounds including pectin, flavonoids, polyphenols, and essential oils (Sharma *et al*., 2017). Along with apple pomace, citrus peel is a major source of pectin (May, 1990). Pectin is an important anionic natural polymer and also a valuable polysaccharide constituent of plant cell wall (Rakhshaee and Panahandeh, 2011) (Fig. 1). The anionic pectin polymer has the main role of combining with the cationic CRV dye

through electrostatics attraction for the adsorption of the dye molecule. Given the above facts, the present study was undertaken with the main objective of exploring the feasibility and application of pectin membrane (PMB) isolated from tangerine for the adsorptive removal of CRV dye. In probing the adsorption behaviour of CV onto PMB, different parameters were systematically evaluated, including kinetics, dye concentration, thermodynamics, as well as isothermal behaviour of the sorption process. The surface morphologies by Scanning Electron Microscope (SEM); crystal structures by X-ray diffraction (XRD); functional groups by Fourier infrared spectroscopy (FTIR) of the PMB before and after CV adsorption were also examined. The adsorption capacity of CV on PMB was then compared with different biosorbent materials that had been applied as adsorbents to remove dyes by different researchers.

Materials and Methods

Material

Crystal violet $[MF = C_{25}N_3H_{30}Cl]$ was procured from Sigma-Aldrich (Steinheim, Germany); the ethanol used was a product of BDH chemicals Ltd (Poole, England); Distilled water (DW) was supplied by the material preparatory unit of our department; Fresh tangerine fruits were sourced from a local fruits market in Ile-Ife, South-West, Nigeria.

Adsorbent preparation and its yield

To prepare the pectin adsorbent, a slightly modified form of the method described by Ghoshal and Negi (2020) was adopted. Each of the fruits was first sliced into two for easy separation of the skin (peels) from the endocarp (the edible parts). The peels were further cut into smaller pieces of about 4x4 cm, and then thoroughly washed under a clean running water (to remove glycosides and possible adhering residues of pesticide spray). Afterwards, the peels were sun-dried until they became crispy. This was followed by pulverization using a domestic mixer/grinder. The pulverized peels, thereafter tagged tangerine peel powder (TPP) were subsequently stored in a tightly covered plastic container to prevent air and moisture access. A quantity (100 g) of this TPP was taken and transferred into a beaker (1000 mL) containing 350 mL DW. The pH of the suspension was adjusted to 5.0, (using 0.1 M HCl); followed by heating on a hot plate stirring module at $90\ ^{\circ}\mathrm{C}$ for 1 h. The suspension was allowed to gradually cool down at room temperature and then filtered with a filter paper. Ethanol was added to the filtrate, in a ratio 6:5 (ethanol: filtrate) proportion with stirring. The solution was left overnight at room temperature to allow the floatation of pectin. The floating pectin gel was isolated by filtration, oven-dried at $40\ ^{\circ}\mathrm{C}$, and crushed. The resulting coarse powder was sieved through a 212 μm mesh, and then stored for subsequent use as an adsorbent; while TPP was used as a control.

The percent pectin yield (wt %) and the e factor were estimated using eqs 1 and 2:

$$Pectin\ yield\ (wt\ \%) = \frac{pectin\ (g)}{raw\ materials\ (g)} \times 100 \quad (1)$$

$$e\ factor = \frac{\mathcal{G}waste}{\mathcal{G}product} \quad (2)$$

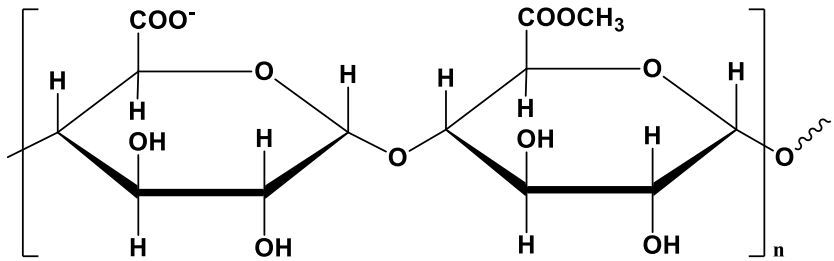

Figure 1: Chemical structure of pectin polymer

Characterization

The crystal structures of the materials (TPP and the extracted pectin) were analyzed by X-ray diffraction spectrometer with a Cu Kα radiation source (Bruker D8 Advance, Germany) in a range of 2θ = 5–90 Å (θ is the diffraction angle) with a scan speed of 5° per minute. Their surface morphologies were investigated using a FEGSEM, 6100 Zeiss Ultra Plus Model. The images were taken at a voltage of 20 kV, while keeping secondary electrons in a low vacuum mode. Functional groups were identified by FTIR Nicolet 330 spectrometer (Thermo Fisher Scientific, USA) in the frequency range of 500 to 4 000 cm^{-1}.

Batch adsorption of crystal violet

Adsorption of the dye (CV) dye was performed, by batch experimental technique, on a GFL thermostatic shaking water bath (Burgwedel, Germany). Influences of factors such as solution pH (in the range of 1–9), contact (agitation) time (5 – 220 min), initial CV concentration (50 – 250 mg/L), and temperature (from 40°C – 70°C) on the adhesion of CV on PMBs were considered. For the determination of optimum pH, series of 20 mL of 100 mg/L CV solution (adjusted to different pHs, ranging from 1–9, in triplicate) were placed in different capped plastic sample containers. pH adjustment was performed with 0.1–1.0 mol/L of either or both HCl and NaOH (as applicable). Upon the placement of 50 mg PMB into each of the solutions whose pHs had been adjusted, the containers were arranged in a shaker and allowed to agitate for 1 h. Separation of the supernatants was performed by centrifugation for 5 min at 6000 r/min. The residual CV concentration in the various supernatants was determined with a spectrophotometer (Shimadzu UV-Vis-1800 model, Canby, Oregon, USA). Wavelength of measurement was set at 590 nm. Studies on the effects of other parameters at the established optimum pH were similarly carried out by varying the parameter under investigation while keeping others constant, preferably at their optimum values if earlier determined, or arbitrary values if not yet determined or not

required. Control experiments were similarly conducted using TPP as the adsorbent. The reusability of PMB was investigated with four cycles of repeated adsorption–desorption experiments. Desorption experiment was performed with 0.01 M HCl as the desorbing agent. The quantity of CV removed (mg/g) and the dye adsorption efficiency were calculated using Eqs (3) and (4), respectively:

$$q_e = \frac{(C_0 - C_e)V}{m} \quad (3)$$

$$E = \frac{C_o - C_e}{C_O} \times 100 \quad (4)$$

Where: q_e stands for dye uptake in mg/g; E stands for adsorption efficiency; C_0 and C_e respectively stand for initial and equilibrium CV concentrations in mg/L; m stands for mass of PMB or TPP in g; V stands for volume of CV solution in L.

Kinetic, isothermal, and thermodynamic modeling

For better understanding of the CV removal process, experimental data were slotted into various model equations. The equations considered include those of kinetic models: pseudo-first-order (Lagergren, 1898), pseudo-second-order (Ho and McKay, 1999), Weber-Morris (W-M) (Weber and Morris, 1963), and Elovich (Cheung et al., 2000); isothermal models: Langmuir (Langmuir, 1918), Freundlich (Freundlich, 1906), and Dubinin–Radushkevich (D-R) (Dubinin et al., 1947; Singh and Mishra, 2010); and the van't Hoff thermodynamic equation expressed in eq. 5.

$$\ln K_c = \frac{\Delta G}{R} - \frac{\Delta H}{RT} \quad (5)$$

Where: K_c, the equilibrium constant, is given as $\frac{C_a}{C_e}$ (C_e represents the residual concentration in solution at equilibrium, while C_a denotes CV concentration taken up by the adsorbent at equilibrium); $\Delta H°$ and $\Delta S°$ respectively represent the standard enthalpy and entropy changes of the process; $\Delta G°$, expressed as $\Delta H - T\Delta S$, stands for the standard Gibb's free energy change; R (with a constant value of 8.314 kJ mol^{-1} K^{-1}) represents gas constant; whereas T (expressed in Kelvin, K) stands for temperature.

Results and Discussion

Morphological, chemical and crystal characterization results

The isolated PMB and the TPP were well characterized via diverse analyses. Fig. 2A shows the morphologies of TPP and PMB before adsorption and after the adsorption of CV

($PMB_{Before}\ and\ PMB_{After}$). The surface of TPP reveals an obvious heterogeneous geometry with rough texture which might be due to the amorphous nature of TPP sample (Singh and Mishra, 2022). Whilst the surfaces of the $PMB_{Before}\ and\ PMB_{After}$ show well-defined network of filamentous structures, typical of pectin (Mamiru and Gonfa, 2023) with PMB_{After} showing a slightly rougher surface compared to PMB_{Before}. This observation suggests that CV molecules most possibly bonded (covalently or via van d der Waals forces) with certain species present at the surface of PMB during the adsorption process. The XRD patterns of $PMB_{Before}\ and\ PMB_{After}$ are shown in Fig. 2B, along with that of TPP for comparison. All the three XRD spectra generally showed amorphous characteristics; although crystallinity slightly improved for the PMBs. As against the pattern shown for TPP, a minor peak at 2θ diffraction peak of $10.13°$ was detected for the PMBs. This finding revealed that even though an increase in semi-crystalline or crystalline properties were observed for the PMBs compared to TPP, the adsorption of the synthetic dye did not alter the crystal structure of the pectin membrane. The FTIR spectra of TPP, $PMB_{Before}\ and\ PMB_{After}$ are shown in Fig. 2C. The FTIR spectra of the $PMB_{Before}\ and\ PMB_{After}$ exhibited similar features, except for the broad band around $3433\ cm^{-1}$ noticed in the spectrum of PMB_{After}. This new peak that appeared after adsorption possibly confirms the presence of -*NH* group from the amine group of CV. In general, the main active functional group in pectin is $-COOH\ or\ COO^{-}$ group, which can be clearly seen at $1492 - 1801\ cm^{-1}$ in the spectra of both PMBs. The PMB spectra also showed broad bands between $906 - 1327\ cm^{-1}$ which can be attributed to the $R - O - R$ of ether and cyclic ring $C - C$ linkages (Liu et al., 2010) in pectin structure. Overall, the presence of $-COOH\ or\ COO^{-}$ group in the pectin presents the biomaterial as a potential adsorbent for the possible sequestration of toxic compounds from wastewaters. The FTIR spectrum of TPP showed completely different FTIR peaks. This indicates that the structure of TPP is entirely distinct from the pectin structure.

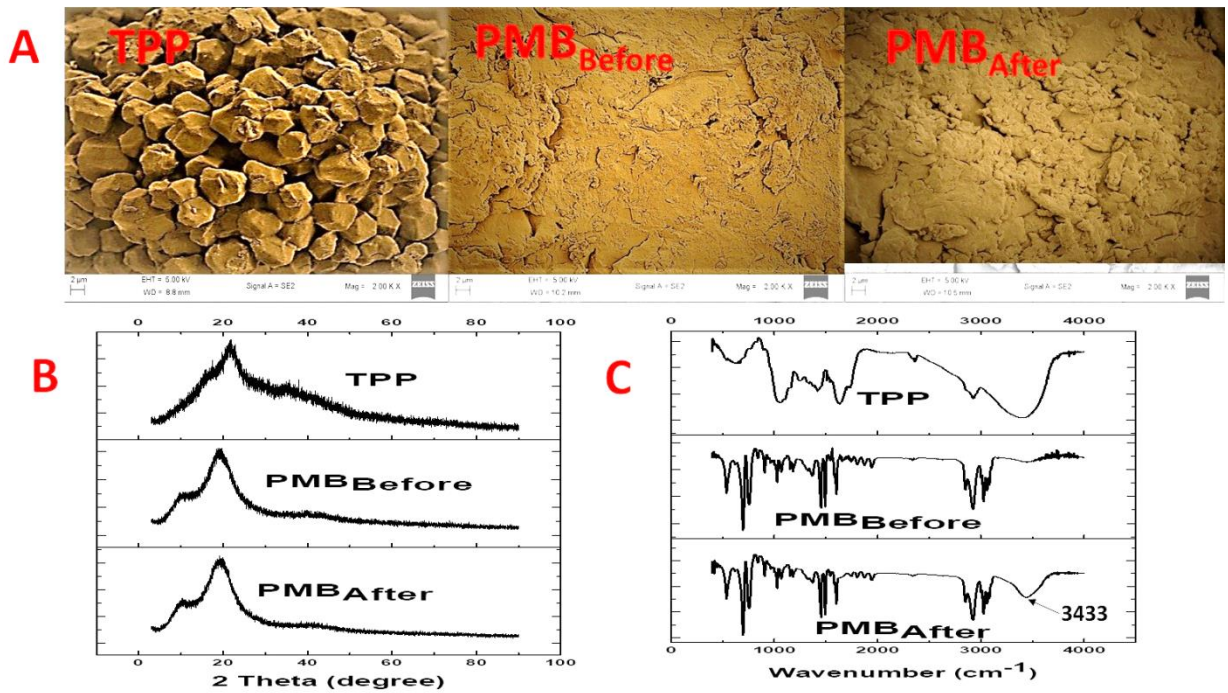

Figure 2: SEM images of the adsorbents (**A**), X-ray diffraction patterns (**B**) and FTIR spectra (**C**)

Pectin yield

The yield of pectin isolated from the TPP sample was 15.29%. This value is higher than the yields reported for tangerine (12.82%) by Hannington *et al*. (2020), and orange (14.53%) by Fakayode and Abobi, (2018). The differences in the yield reported here and those earlier reported could be due to the nature of the fruits and/or the differences in the extraction process (i.e processing conditions: pH, extraction time, temperature etc) (Fakayode and Abobi, 2018). In addition, the ***e-factor***, is a common measure of how "green" a process is. For instance, a chemical reaction may have 100% yield, but still generate more waste than the product. The ***e-factor*** has been calculated to be 30.46. This clearly shows the existence of a vast number of by-products (include cellulose) from the solid residue (Ghoshal and Negi, 2020).

Adsorption of CV

pH effect and kinetics of the process

A crucial influencing factor in an adsorption process is solution pH. The pH of the solution influences the surface functionality of adsorbents, along with the degree of ionization or dissociation of the contaminant's molecules (Markandeya et al., 2017). Fig. 3a depicts the effect of pH on the adhesion of CV on PMB/TPP. The efficiency of the adsorbents in

removing CV was observed to increase from 98.07 to 99.83% (with PMB as adsorbent), and 49.04 to 49.92% (with TPP as adsorbent) upon increasing pH from 1 to 4. However, at pH beyond 4, the removal efficiency decreased, with the lowest values of 95.66% (for CV-PMB interaction) and 47.83% (for CV-TPP interaction) recorded at pH 9. The optimum adsorption recorded at pH 4 (acidic medium) could be due to strong attractive forces between the negatively charged PMB surface and the cationic CV molecules (Loulidi et al., 2020). Effect of contact time on the adsorption process (studied from 5 – 220 min) is shown in Fig. 3b. The obtained result showed a rapid increase in CV uptake within the first 20 min of contact. Equilibrium uptake was eventually reached after 60 min. At equilibrium, about 98.3 and 43.1% CV was adsorbed by PMB and TPP, respectively. The fast CV uptake observed within the first 20 min, especially in the presence of PMB, could be attributed to the accessibility of the CV molecules to a great number of vacant active sites present at the adsorbent's surface. The parameters obtained from modelling the kinetics of the CV adsorption process are recorded in Table 1. The values of the determination coefficient, R^2 obtained for the ***PSO*** $(R^2 = 1.000\ for\ both\ PMB\ and\ TPP)$ indicates the superiority of the PSO model in describing the adsorption process. This submission was supported by the closeness of the calculated q_e ***values*** $(7.9643\ mg\ g^{-1}\ for\ PMB)$ $and\ (5.1267\ mg\ g^{-1}\ for\ TPP)$ to the experimental q_e ***values*** $(7.8678\ mg\ g^{-1}\ for\ PMB)$ $and\ (5.0945\ mg\ g^{-1}\ for\ TPP)$. This kinetic behavior is indicative of chemisorption being the rate-determining step when considering the mechanism of the CV removal process. Hence, the adsorption process most possibly involved the exchange of valency forces amongst the adsorbents and CV molecules (Jawad et al., 2022; Eldeeb et al., 2022a; Sterenzon et al., 2022). This finding is in line with those previously reported for the adsorption of CV onto the surface of other adsorbents (Foroutan et al., 2021; Sulthana et al., 2022). The Elovich model often provides crucial information about the chemical nature of the adsorption process, together with the connection between activation energy and the extent of surface coverage (Mahmoud et al., 2022). The $\propto$ parameter (calculated from Elovich model)) recorded for $PMB\,(3.1\mathrm{E}+3)$ was found to be higher than that of $TPP\,(2.3\mathrm{E}+3)$, showing that PMB had a greater uptake of CV dye compared to TPP (Foroutan et al., 2021). The Weber-Morris intraparticle diffusion model is usually used to describe diverse stages in an adsorption process. In this study, the intercept (C) on the vertical axis of the W-M plot respectively occurred at 13.17 mg g^{-1} and 11.29 mg g^{-1} for PMB and TPP. The deviation of the intercept from the origin is an indication of intraparticle step not being the sole mechanism step controlling the adsorption process (Dotto and Pinto, 2012).

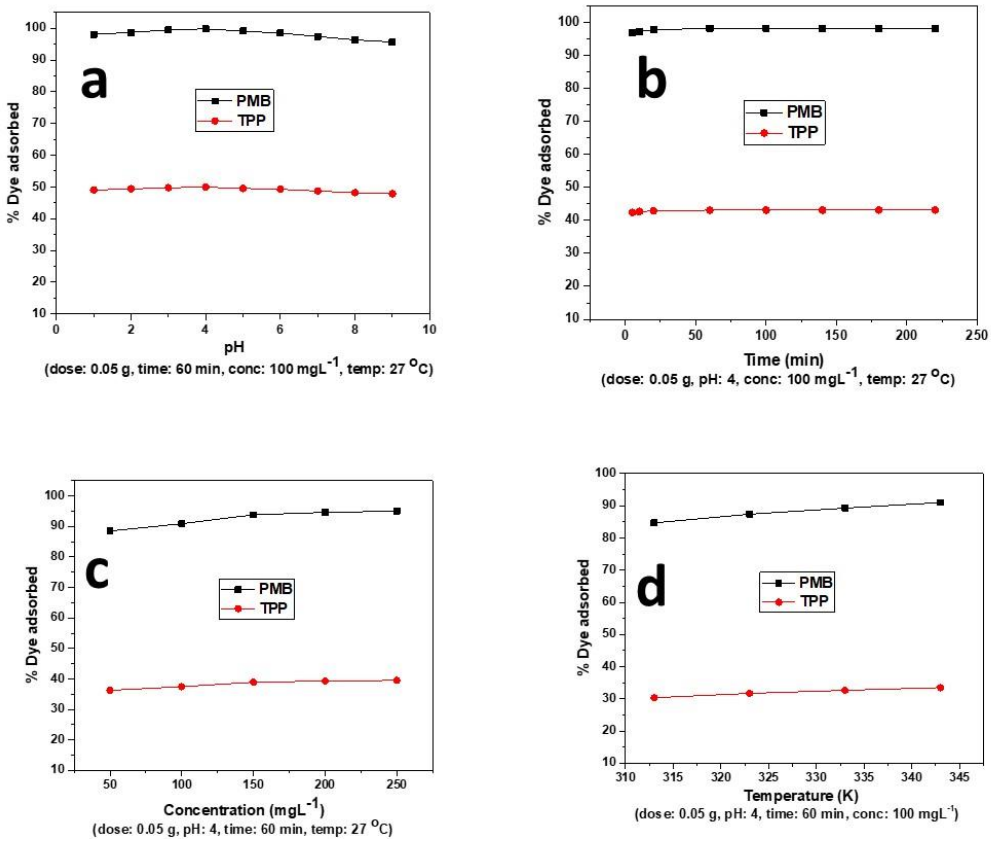

Fig.3 *Plots of the effects of* (a) *pH,* (b)*contact time,* (c) *initial concentration, and* (d) *temperature on the adsorption of CVby* ***PMB/TPP***

Table 1: Equations of Different Kinetic Models and Their Calculated Parameters for the Adsorption of CV onto PMB and TPP

Model	**Equation**	**Parameter**	**PMB**	**TPP**	**Definition of parameter**
PFO	$\ln(q_e - q_t) = \ln q_e - k_1 t$	R^2	0.6545	0.3113	q_t: amount of dye adsorbed
		k_1 (L/min)	0.0188	0.0102	k_1: PFO rate constant
		$q_{e(exp)}$ (mg/g)	0.0442	1.0032	t: time
		$q_{e(calc)}$ (mg/g)	11.967	13.007	
PSO	$\frac{t}{q_t} = \frac{t}{q_e} - \frac{1}{k_2 q_e^2}$	R^2	1.0000	1.0000	K_2: PSO rate constant

		k_2 (g/mg.min)	1.5535	1.3421	
		$q_{e(exp)}$ (mg/g)	7.8678	5.0945	
		$q_{e(cal)}$ (mg/g)	7.9643	5.1267	
W-M	$q_t = k_\alpha t^{½} + C$	R^2	0.9787	0.9695	k_α: W-M rate constant
		k_α (mg/g. $min^{½}$)	0.5896	0.2763	C: intercept
		C	13.172	11.297	
Elovich	$q_t = \frac{1}{\beta}\ln[\alpha\beta] + \frac{1}{\beta}\ln t$	R^2	0.8608	0.8342	α: initial adsorption rate
		α (mg/g. min)	3.1E+3	2.3E+3	β: desorption constant
		B	31.153	29.133	

Influence of concentration on the removal of CV

The influence of CV concentration on its sequestration was evaluated by varying CV concentrations within the range of $50 - 250\,mgL^{-1}$ as depicted graphically in Fig. 3c. CV uptake augmented with increasing initial CV concentration up to $150\,mgL^{-1}$ in an almost linear manner. With CV concentration of $150\,mgL^{-1}$, about 93.8% and 38.9% dye removal efficiency was recorded for CV adsorption onto PMB and TPP, respectively. Beyond $150\,mgL^{-1}$, CV uptake slowed down up to $250\,mgL^{-1}$, the highest concentration investigated. At $250\,mgL^{-1}$, about 95.1% and 39.5% PMB and TPP were respectively adsorbed. The near constant CV uptake recorded from $200 - 250\,mgL^{-1}$ CV concentration might possibly be as a result of almost complete occupation of the binding sites on the PMB and TPP adsorbents (Smith et al., 1990). As observed for both pH and time dependent studies, in all the concentrations considered, PMB was found to be more efficiencies than TPP. This reveals that the anionic PMB surface had higher affinity for the cationic CV dye molecule.

Adsorbent isotherms

To describe the adsorption mechanism, equilibrium data were fitted to the Dubinin–Radushkevich (D-R), Langmuir, and Freundlich isotherm equations. Table 2 shows the calculated parameters from the various models. Due to the highest R^2 values obtained ($R^2 = 0.9692\ for\ PMB\ and\ 0.9734\ for\ TPP$), the Freundlich model was found to be most appropriate in describing the adsorption of CV on both adsorbents. The Freundlich heterogeneity factor, n, which indicates the adsorption intensity/strength, was found to be less than unity for both PMB (0.8226) and TPP (0.2786). This suggests that the mechanism

of the adsorption process probably involved chemisorption, corroborating the results of the kinetic study (Sadegh et al., 2021). In addition, the higher n value of PMB compared to TPP reveals a better affinity of pectin for the dye. For the Langmuir model, TPP showed a lower q_m value of 13.554 $mg\ g^{-1}$ compared to PMB with q_m value of 133.69 $mg\ g^{-1}$. The higher q_m value for PMB might be as a result of its affinity for CV and possible availability/exposure of more active sites for the binding of target molecules. In comparison with the efficiencies of other adsorbents reported in the literature, Table 3 shows that the value of q_m obtained for this present study $(133.69\ mg\ g^{-1})$ is far higher than those reported for any other adsorbent in the removal of CV. This study shows that the PMB used here was possibly very rich in functional group acting as binding sites for the target CV molecules. The calculated mean free energy values (from D–R model) were found to be 34.00 and 9.15 kJ mol^{-1} for PMB and TPP, respectively. The E values, being $> 8\ kJ\ mol^{-1}$ indicate that chemical adsorption played a predominant role during the CV removal process (Awokoya et al., 2021).

Table 2: Isothermal Equations and the Calculated Values of their Parameters

Model	**Equation**	**Parameter**	***PMB***	***TPP***
Langmuir	$\frac{1}{q_e} = \frac{1}{q_{max} K_{LC_e}} + \frac{1}{q_{max}}$	R^2	0.9158	0.8963
		$k_L\ (L\ mg^{-1})$	0.0949	0.0700
		$q_{max}(mg\ g^{-1})$	133.69	13.554
Freundlich	$\ln q_e = \ln k_f + \frac{1}{n} \ln C_e$	R^2	0.9692	0.9734
		$k_F\ (L\ mg^{-1})$	0.0154	0.0127
		n	0.8226	0.2786
D-R	$\ln q_e = \ln q_m - \beta\varepsilon^2$	R^2	0.9261	0.8817
		$q_m(mmol\ g^{-1})$	96.824	73.442
		$E\ (kJ\ mol^{-1})$	34.003	9.1457

Table 3: Comparison of Langmuir Adsorption Capacity of PMB used in this Study with some Selected Biosorbent Materials

Material	**Dose (g)**	$\boldsymbol{Conc\ (mg\ L^{-1})}$	$\boldsymbol{q_{max}\ (mg\ g^{-1})}$	
			CV	
This study	0.05	$50 - 250$	133.69	
Sugarcane bagassee	*0.2*	$5 - 30$	2.94	(Mahdi et al. 2023)
Peanut husk	*0.5*	$100 - 450$	20.95	(Abbas et al. 2021)
Raw chitin	*0.80*	30	-10.80	(Sadoq et al., 2024)
Charrred rice husk	*0.025*	$20 - 1000$	62.85	(Homagai et al. 2022)

Effect of temperature variation and the thermodynamics of the process
Further prediction of the nature of the adsorption of CV onto PMB/TPP as well as the determination of the thermodynamic parameters (such as ΔGº, ΔH° and ΔS°) associated with the process were performed by studying the effect of temperature on the dye uptake within $40 - 70°C$ temperature range. The result is graphically presented in Fig. 3d. CV uptake increased with temperature rise: adsorption of CV increased from 84.19 to 91.02%, and 30.35 to 33.51% with PMB and TPP adsorbents, respectively, as the medium temperature was increased from $40 - 70°C$. This suggests an endothermic process. A similar adsorption nature was reported for the adsorption of malachite green dye onto *Ni/NiO* nanoparticles (Abukhadra et al. 2019). As depicted in Table 4, ΔH° and ΔS° of the process were positive, while ΔGº was negative. The positive value of ΔH° further confirms an endothermic process. The values of ΔS° obtained as $+0.0704\ kJmol^{-1}$ for PMB and $+0.0617\ kJmol^{-1}$ for TPP suggest a process that occurred with increasing randomness or disorderliness at the CV- adsorbent interface (Sulthana et al., 2022). The negative ΔGº values for all the temperatures which decreased with rise in temperature indicates a spontaneous interaction. Also, the decrement in the value of ΔGº (with temperature rise) strongly suggests an enhanced CV adsorption with rise in temperature, indicating a more favorable process at elevated temperature (Sulthana et al., 2022; Oninla et al., 2022).

Table 4: Values of Thermodynamic Parameters Calculated for the Adsorption of CV onto *PMB/TPP*

Parameter	Definition	Temp (K)	PMB	TPP
ΔH° (kJ/mol)	Standard enthalpy change		17.66	17.56
ΔS° (kJ/mol)	Standard entropy change		0.0704	0.0617
ΔG° (kJ/mol)	Standard Gibb's free energy change	313	–4.446	–1.7614
		323	–5.149	–2.3784
		333	–5.854	–2.9954
		343	–6.558	–3.6124

Regeneration studies
The possibility of regeneration/reusability of PMB, like any other adsorbent, would be a vital and remarkable factor to be considered for its practical/industrial applications and economic viability. Regeneration of PMB was performed in four adsorption-desorption cycles with 0.01 M HCl solution at room temperature. As depicted in Fig. 4, 95.04% efficiency was achieved within the first three cycles. However, at the fourth cycle,

adsorption efficiency slightly decreased by 1.56%. This result clearly shows the economic viability of PMB, coupled with its high efficiency earlier determined.

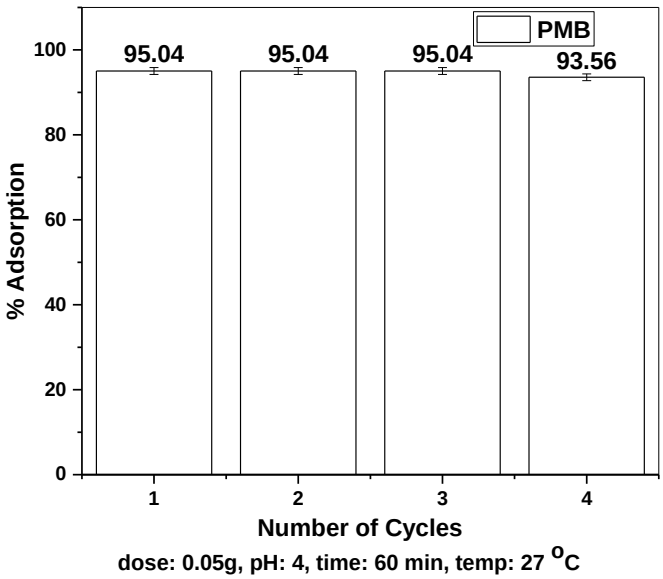

Figure 4: Reusability study for the adsorption of crystal violet

Method validation

The method validation was performed by applying the PMB adsorbent to treat real industrial wastewater sample (collected from Ibadan city, Nigeria). The results showed that the amount of CV adsorbed from the wastewater was about 82.33%. The results suggest that PMB adsorbent had remarkable stability in real matrix and can be used for further dye adsorption on an industrial scale.

Conclusion

This study showed the potentials of pectin isolated from tangerine peels in the removal of CV from aqueous medium. Morphological investigation revealed that CV molecules were bound to the surface of PMB after adsorption, while XRD analysis showed that the adsorption of CV did not alter the crystal structure of the pectin membrane. FTIR investigation revealed the main active functional group in pectin to be $-COOH\ or\ COO^{-}$. A maximum CV adsorption capacity, q_{max} of $133.69\ mg\ g^{-1}$ was achieved by PMB. This

value appears very high when compared with values reported for other adsorbents in the literature. The adsorption of CV dye on PMB was preferentially defined by Freundlich and PSO isotherm and kinetic models, respectively. The adsorption of CV was a fast process, in which more than 96% CV became adhered to the surface of PMB within the first 20 min of contact. CV was presumed to be adsorbed onto PMB via electrostatic interactions. Thermodynamic analysis showed that the adsorption of CV was characteristically spontaneous and endothermic. Upon regeneration, the reusability efficacy of the pectin was more than 90% up to four adsorption-desorption cycles. It can then be concluded that the use of pectin isolated from agricultural wastes such as tangerine peels as biosorbent is very viable and economical.

References

Abbas, S., Javeed, T., Zafar, S., Taj, M.B., Ashraf, A.R. and Din, M.I. (2021). Adsorption of crystal violet dye by using a low-cost adsorbent – peanut husk. *Desalination and Water Treatment,* 233: 387–398.

Abukhadra, M.R., Sayed, M.A., Rabie, A.M. and Ahmed,S.A. (2019). Surface decoration of diatomite by Ni/NiO nanoparticles as hybrid composite of enhanced adsorption properties for malachite green dye and hexavalent chromium, *Colloids Surfaces A Physicochemical and Engineering Aspects* 577: 583–593,

Auerbach, S.S., Bristol, D.W., Peckham, J.C., Travlos, G.S., Hebert, C.D., and Chhabra, R.S. (2010). Toxicity and carcinogenicity studies of methylene blue trihydrate in F344N rats and B6C3F1 mice. *Food Chem Toxicol.* 48(1):169–177.

Awokoya, K. N., Oninla, V. O., Adeyinka, G. C., Ajadi, M. O., Chidimma, O. T., Fakola, E. G. and Akinyele, O. F. (2022). Experimental and computational studies of microwave-assisted watermelon rind–styrene based molecular imprinted polymer for the removal of malachite green from aqueous solution. *Scientific African 16*: e01194.

Awokoya, K. N., Oninla, V. O. and Bello, D. J. (2021). Synthesis of oxidized *Dioscorea dumentorum* starch nanoparticles for the adsorption of lead (II) and cadmium II) ions from [Environ. Nanotechnol. Monit. Manage. *Wastewater Environmental Nanotechnology, Monitoring & Management, 16*: 100489.

Awokoya, K.N., Batlokwa, B.S, Moronkola, B.A., Chigome, S., Ondigo, D.A., Tshentu, Z. and Torto, N. (2013). Development of a styrene based molecularly imprinted polymer and its molecular recognition properties of vanadyl tetraphenylporphyrin in organic media. *International Journal of Polymeric Materials and Polymeric Biomaterials,* 63: 1077-1133.

Babu, B. R., Parande, A. K., Raghu, S. and Kumar, T. P. (2007). Textile technology. Cotton textile processing: Waste generation and effluent treatment. *Journal of Cotton Science*, *11*: 141–153.

Basheer, A. A. and Ali, I. (2018). Stereoselective uptake and degradation of (±)-o, p-DDD

pesticide stereomers in water-sediment system. *Chirality*, 30: 1088–1095.

Bautista, P., Mohedano, A. F., Gilarranz, M. A., Casas, J. A. and Rodriguez, J. J. (2007). Application of Fenton oxidation to cosmetic wastewaters treatment. *Journal of Hazardous Materials*, 143: 128–134.

Burakov, A.E., Galunin, E.V., Burakova, I.V., Kucherova, A.E., Agarwal, S., Tkachev, A. G. and Gupta, V.K., (2018). Adsorption of heavy metals on conventional and nanostructured materials for wastewater treatment purposes: a review. *Ecotoxicol. Ecotoxicology and Environmental Safety* 148: 702–712.

Cheung, C. W., Porter, J. F. and McKay, G. (2000). Elovich equation and modified second-order equation for sorption of cadmium ions onto bone char. *Journal of Chemical Technology & Biotechnology 75*: 963-970.

Dotto, G. L. and Pinto, L. A. A. (2012). Analysis of mass transfer kinetics in the biosorption of synthetic dyes onto *Spirulina platensis* nanoparticles. *Biochemical Engineering Journal*, *68*: 85–90.

Dubinin, M. M., Zaverina, E. and Radushkevich, L. (1947). Sorption and structure of active carbons. Adsorption of organic vapors. *Zhurnal Fizicheskoi Khimii* 21(3): 151-162.

Eldeeb, T.M., Aigbe, U.O., Ukhurebor, K.E., Onyancha, R.B., El-Nemr, M.A., Hassaan, M.A., Ragab, S., Osibote O.A. and El Nemr, A. (2022). Adsorption of methylene blue (MB) dye on ozone, purified and sonicated sawdust biochars. *Biomass Biomass Conversion Biorefinery* 1–23. https:// doi. org/10.1007/ s13399- 022-03015-w

Fakayode, O.A. and Abobi, K.E. (2018). Optimization of oil and pectin extraction from orange (*Citrus sinensis*) peels: a response surface approach. *Journal of Analytical Science and Technology*, 9: 20.

Freundlich, H.M., 1906. Uber die adsorption in lasungen. Z. Phys. Chem. 57: 385–470

Foroutan, R., Peighambardoust, S.J., Peighambardoust, S.H., Mirian Pateiro, M. and Lorenzo, J.M. (2021). Adsorption of crystal violet dye using activated carbon of lemon wood and activated carbon/fe3o4 magnetic nanocomposite from aqueous solutions: a kinetic, equilibrium and thermodynamic study. *Molecules*, 26: 2241.

Ghoshal, G. and Negi, P. (2020). Isolation of pectin from kinnow peels and its characterization. *Food and Bioproducts Processing*, 124(2): 342-353.

Hamad, H.N. and Idrus, S. (2022). Recent developments in the application of bio-waste-derived adsorbents for the removal of methylene blue from wastewater: a review. *Polymers*, 14: 783.

Hannington, T., Awuchi, C. G. and Daphine K. (2020). Extraction and characterization of pectin from orange (citrus sinensis), lemon *(Citrus limon)* and tangerine (*Citrus tangerina*). *American Journal of Physical Sciences* 1: 17 – 30.

Ho, Y.S. and McKay, G. (1999). Pseudo-second order model for sorption processes. *Process Biochemistry* 34(5): 451–465.

Kaushal, A. and Singh, S.K. (2017). Removal of heavy metals by nanoadsorbents: a review.

Journal of Environment &. Biotechnoogy 6: 96–104.

Jawad, A.H., Saber, S.E., Abdulhameed, A.S., Reghioua, A.L., Othman, A.Z.A. and Wilson, L.D. (2022). Mesoporous activated carbon from mangosteen (*Garcinia mangostana*) peels by H_3PO_4 assisted microwave: optimization, characterization, and adsorption mechanism for methylene blue dye removal. *Diamond & Related Materials* 129:109389.

Lagergren, S. (1898). About the theory of so-called adsorption of soluble substances. Kungliga Svenska Vetenskapsakademiens Handlingar Band, 24: 1–39.

Langmuir, I. (1918). The adsorption of gases on plane surfaces of glass mica and platinum. *Journal of American Chemical Soc*iety 40(9): 13611402.

Liu, L., Cao, J., Huang, J., Cai, Y and Yao, J. (2010). Extraction of pectins with different degrees of esterification from mulberry branch bark. *Bioresource. Technology* 101: 3268–3273.

Loulidi, I., Boukhlifi, F., Ouchabi, M., Amar, A., Jabri, M., Kali, A., Chraibi, S., Hadey, C. and Aziz, F. (2020). Adsorption of crystal violet onto an agricultural waste residue: kinetics, isotherm, thermodynamics, and mechanism of adsorption. *The Scientific World Journal Article* ID 5873521 | https://doi.org/10.1155/2020/5873521

Mahdi, E.R., Shihab, E.A. and Fahmi, A.H. (2023). Crystal violet dye adsorption by biochar produced from sugarcane bagasse under different temperatures. *Passer*, 5: 422-427.

Mahmoud, M.E., El-Sharkawy, R.M. and Ibrahim, G.A.A. (2022). A novel bionanocomposite from doped lipase enzyme into magnetic graphene oxide-immobilized-cellulose for efficient removal of methylene blue and malachite green dyes. *Journal of Molecular Liquids* 368: 120676.

Mamiru, D. and Gonfa, G. (2023). Extraction and characterization of pectin from watermelon rind using acetic acid. *Heliyon*, 9: e13525.

Markandeya, S., Shukla, S.P and Mohan, D. (2017). Toxicity of disperse dyes and its removal from wastewater using various adsorbents: a review. *Research Journal of Environmental Toxicology* 11: 72–89.

May, C. D. (1990). Industrial pectins: sources, production and applications. *Carbohydrate Polymers* 12: 79−99.

Muntean, S.G., Paska, O., Coseri, S, Simu, G.M., Grad, M.E. and Ilia, G. (2013). Evaluation of a functionalized copolymer as adsorbent on direct dyes removal process: kinetics and equilibrium studies. *Journal of Applied Polymer Sci*ence 127(6): 4409–4421.

Noreen, S., Bhatti. H.N., Iqbal, M., Hussain, F. and Sarim, F.M. (2020). Chitosan, starch, polyaniline and polypyrrole biocomposite with sugarcane bagasse for the efficient removal of Acid Black dye. *International Journal of Biological Macromolecules*, 147: 439-452.

Oninla, V. O., Awokoya, K. N., Babalola, J. O., Balogun, K. I. and Ismail, O. S. (2022). Optimization of synthesis conditions for graft copolymerization of methacrylic acid

onto Garcinia kola pods and use in the sequestration of cationic dyes from simulated wastewaters. *Biomass Conversion & Biorefinery* 1-18.

Roohan, R. and Mohammad, P. (2011). Stabilization of a magnetic nano-adsorbent by extracted pectin to remove methylene blue from aqueous solution: A comparative studying between two kinds of cross-likened pectin. *Journal of Hazardous Material*s 189: 158-166.

Sadegh, N., Haddadi, H., Arabkhani, P., Asfaram, A. and Sadegh, F. (2021). Simultaneous elimination of rhodamine B and malachite green dyes from the aqueous sample with magnetic reduced graphene oxide nanocomposite: optimization using experimental design. *Journal of Molecular Liquids* 343: 117710.

Sadoq, M., Atlas, H., Imame, S., Kali, A., Amar, A., Loulidi, I., Jabri, M., Sadoq, B.E., Ouchabi, M., Abdullah, P.S. and Boukhlifi, F. (2024). Elimination of crystal violet from aqueous solution by adsorption on naturel polysaccharide: kinetic, isotherm, thermodynamic studies and mechanism analysis. *Arabian Journal of Chemistry* 17: 105453.

Saini R.D. (2017) Textile organic dyes: polluting effects and elimination methods from textile waste water. *International Journal of Chemical Engineering Research* 9: 121–136.

Salahi, S., Parvini, M. and Ghorbani, M. (2014). Equilibrium studies in adsorption of Hg (II) from aqueous solutions using biocompatible polymeric polypyrrole-chitosan nanocomposite. *Polycyclic Aromatic Compounds* 34: 225–236.

Sharma, K.; Mahato, N.; Cho, M. H. and Lee, Y. R. (2017). Converting citrus wastes into value-added products: economic and environmently friendly approaches. *Nutrition*, 34: 29−46.

Shokrollahi, A., Alizadeh, A., Malekhosseini, Z. and Ranjbar, M. (2011). Removal of bromocresol green from aqueous solution via adsorption on *ziziphus nummularia* as a new, natural, and low-cost adsorbent: kinetic and thermodynamic study of removal process. *Journal of Chemical & Engineering Data* 56: 3738-3746.

Singh, D.K. and Mishra, S. (2010). Synthesis and characterization of Hg(II)-ion-imprinted polymer: kinetic and isotherm studies. *Desalination*, 257: 177–183.

Singh, S. and Mishra, S. (2022). Organoleptic and morphological analysis of citrus peel powder. *European Journal of Food Science and Technology*, 10: 24-38.

Smith, J. A., Jaffe, P. R. and Chiou, C. T. (1990). Effect of ten quaternary ammonium cations on tetrachloromethane sorption to clay from water. *Environmental Science & Technology* 24: 1167– 1172.

Srivastav, A.K. and Roy, D. (2016) Malachite green (triarylmethane dye) and pyceze (bronopol) induced histopathological and biochemical changes in the liver of stinging catfish Heteropneustes fossilis (Bloch, 1794), *Indian Journal of Fish*, 63: 135–139.

Sterenzon, E., Vadivel, V.K., Gerchman, Y., Luxbacher, T., Narayanan, R. and Mamane, H.

(2022). Effective removal of acid dye in synthetic and silk dyeing effluent: isotherm and kinetic studies. *ACS Omega*, 7: 118–128.

Sulthana, R., Taqui, S.N., Syed, U.T., Khan, T.M.Y., Khadar, S.D.A., Mokashi, I., Shahapurkar, K., Kalam, M.A., Murthy, H.C.A. and Syed, A.A. (2022). Adsorption of crystal violet dye from aqueous solution using industrial pepper seed spent: equilibrium, thermodynamic, and kinetic studies. *Adsorption Science & Technology*, Article ID 9009214. https://doi.org/10.1155/2022/9009214.

Wang, J., Da, L., Song, K. and Li, B. L. (2008). Temporal variations of surface water quality in urban, suburban and rural areas during rapid urbanization in Shanghai, China. *Environmental Pollution*, 152: 387–393.

Weber, W.J. and Morris, J.S. (1963). Kinetics of adsorption on carbon from solutions. *Journal of Sanitary Engineering Div*ision, *American Society of Civil Engineers* 89(2): 31–59.

Zewail, T.M. and Yousef, N.S. (2015). Kinetic study of heavy metal ions removal by ion exchange in batch conical air spouted bed. *Alexandria Engineering Journal* 54: 83–90

Zhang, D., Yin, J., Zhao, J., Zhu, H. and Wang, C. (2015). Adsorption and removal of tetracycline from water by petroleum coke-derived highly porous activated carbon. *Journal of Environmental Chemistry and Engineering*, 3: 1504–1512.